Publications

Available Online

J. Sci. Res. **17** (2), 569-586 (2025)

JOURNAL OF SCIENTIFIC RESEARCH

www.banglajol.info/index.php/JSR

Study of 5-Aryl-Furan Derivatives as a Corrosion Inhibitor for Mild Steel in 0.1 N HCl Solution

S. Satarkar*, R. S. Dubey

Chemistry Research Laboratory, Department of Chemistry, R.J College (Autonomous), Ghatkopar (W), Mumbai- 400086, India

Received 2 October 2024, accepted in final revised form 24 February 2025

Abstract

In 0.1 N HCl solution, 5-[4-bromophenyl]-furan-2-carbaldehyde and 5-[4-chlorophenyl]-furan-2-carbaldehyde, two derivatives of furan, were synthesized and used as corrosion inhibitors for mild steel. The effectiveness of the inhibition of both inhibitors was investigated using surface analytical, electrochemical, and gravimetric techniques. It was discovered that both inhibitors' inhibition efficiency increased and their corrosion rate decreased as the quantities of the inhibitors were increased. The maximum inhibitory efficiencies were 92.10 % and 89.47 % for 5-[4-bromophenyl]-furan-2-carbaldehyde and 5-[4-chlorophenyl]-furan-2-carbaldehyde, respectively, at 600 ppm concentration. As the temperature increased, the inhibition effectiveness decreased for both inhibitors. The finding of the electrochemical study that the two inhibitors used are mixed types was supported by both physical and chemical adsorption data. The findings of the gravimetric study best matched the Langmuir Adsorption Isotherm. The results of the gravimetric and electrochemical analyses showed a significant connection. SEM and EDAX studies were used to confirm the passive film that formed on the metal surface.

Keywords: Corrosion; Inhibitors; Furan derivatives.

doi: https://dx.doi.org/10.3329/jsr.v17i2.76595 J. Sci. Res. **17** (2), 569-586 (2025)

1. Introduction

Corrosion refers to the naturally occurring degradation or destruction of metals or other materials as a result of their electrochemical or chemical interaction with their surroundings [1,2]. Many sectors, including those dealing with oil and gas, refineries, and petroleum, have begun to choose mild steel for storage, pipeline, and transportation applications because of its mechanical qualities and strength [2-5]. "However, mild steel is very susceptible to corrosion when it comes into touch with acid solutions. This happens in a variety of industrial contexts, including acid descaling, storage, transportation, and acid

* *Corresponding author*: sahilsatarkar@gmail.com

cleaning [2-6]. Mild steel corrosion undermines safety precautions, leads to expensive maintenance, and reduces product value, all of which lead to economic losses [7].

Methods such as anodic protection, cathodic protection, inhibitor usage, and protective coating application are among those being investigated. However, because of their cheap cost, quick availability, and great efficacy, inhibitors are the most often used preventative approach [4]. The majority of acid solution inhibitors are organic substances. The metal surface becomes impermeable to acidic fluids due to the adsorption of these inhibitors. Organic molecules, cyclic rings and conjugate systems, as well as heteroatoms such as O, N, P, and S, make the adsorption a realistic possibility. Organic inhibitors may either physically or chemically adsorb to metal surfaces, where they then create a protective coating. The metal is protected against corrosion by organic inhibitors because they either obstruct the surface-active sites or slow down the electrochemical action [6-11].

Oxygen is a heteroatom in the five-membered heterocyclic ring furan. It finds extensive use in the pharmaceutical sector. One of the many uses for furan derivatives is as a reagent in the treatment of several diseases and conditions, including inflammation, pain, depression, parkinsonism, and muscle relaxation [12,13]. Furan derivatives are effective corrosion inhibitors because the oxygen heteroatoms on them allow them to be adsorbed onto metal surfaces. These considerations have led to a number of investigations into the potential of furan derivatives as acidic-medium corrosion inhibitors for mild steel.

Ali *et al*. studied the corrosion inhibition of synthesized furan derivatives namely 5((5(3,4,5 trimethoxyphenyl)furan2yl)methylene)pyrimidine 2,4,6 (1H,3H,5H) trione (HM-1221), 2 thioxo5((5 (3,4,5 trimethoxyphenyl)furan2yl)methylene) dihydropyrimidine 4,6(1H,5H)dione(HM-1222), 1,3 diethyl 2 thioxo 5 ((5(3,4,5 trimethoxyphenyl)furan2yl) methylene)dihydropyrimidine 4,6(1H,5H)dione (HM-1223) and 1,3 dimethyl 5((5(3,4,5 trimethoxyphenyl)furan2yl) methylene)pyrimidine 2,4,6(1H,3H,5H)trione (HM-1224) for mild steel in acidic conditions. The corrosion testing was conducted using electrochemical analytical methods and the weight loss method. Compound HM-1223 had a maximal inhibitory effectiveness of 92.9 % at a concentration of 11×10^{-6} M [14]. The efficiency of 2-furanmethanethiol (FMT) and 2-furonitrile (FN) as corrosion inhibitors for mild steel in acidic conditions was examined by Al-Fakih *et al*. To evaluate the inhibitory efficacy of the furan derivatives under study, researchers used weight loss analysis in conjunction with electrochemical analysis. A concentration of 0.005 M resulted in a 94 % inhibitory effectiveness for FMT [15]. Researchers have looked at furan derivatives, however they've mostly focused on less acidic concentrations. In view of the above, it is critical to use furan derivatives at somewhat greater acidic concentrations. So, we're making a real attempt to create furan derivatives that are both inexpensive and environmentally acceptable so that we may use them to protect mild steel from corrosion in an acidic solution (0.1 N).

This study details the effectiveness of two synthetic furan derivatives in inhibiting corrosion: 5-[4-chlorophenyl]-furan-2-carbaldehyde (CFC) and 5-[4-bromophenyl]-furan-2-carbaldehyde (BFC). Researchers examined the inhibitors' corrosion-inhibiting properties at ambient temperature and elevated temperatures using gravimetric analysis, a method analogous to the weight loss approach. Electrochemical techniques, including

potentiodynamic polarization methods and open circuit potentials (OCP), were employed to investigate the inhibitors' inhibitory effects. The adsorbed coating that formed on the metal surface was studied with scanning electron microscopy (SEM) and energy-dispersive X-ray analysis (EDAX).

2. Experimental Procedure

2.1. *Material and sample preparation*

The mild steel utilized for all gravimetric and electrochemical experiments had the following composition: C-0.16 %, Si-0.10 %, Mn-0.40 %, P-0.013 %, Si-0.02 %, and the other components were iron. Rectangular coupons of 1 cm × 3.5 cm × 0.020 cm were used to sample the mild steel. The mild steel was prepared for use in experiments by first abrading its surface using emery paper nos. 60, 80, 100, 120, 150, and 220, followed by a rinse in acetone and room-temperature drying in a desiccator.

2.2. *Inhibitors and solutions*

Using double-distilled water to dilute analytical-grade 36 % HCl, a 0.1 N HCl solution was created for use as a hostile medium. Both the acid solution for electrochemical analysis and weight loss were tested with and without various amounts of inhibitors that were synthesized.

2.3. *Synthesis*

0.01 mol of substituted aniline was dissolved in a mixture of conc. HCl and 20 cm^3 water while constant stirring, the solution was cooled to -5 °C in an ice bath. A solution of sodium nitrite was added portion-wise, keeping the temperature below 8 °C. The reaction mixture was left for one hour to complete diazotization. The solution was filtered. The filtered solution was added dropwise to a solution of furfural (2 cm^3 furfural in 10 cm^3 of acetone and water), followed by the solution of copper chloride. The obtained solution was stirred at room temperature for 6 h and then left for 24 h. The obtained precipitate was filtered, dried and recrystallized by ethanol [16,17].

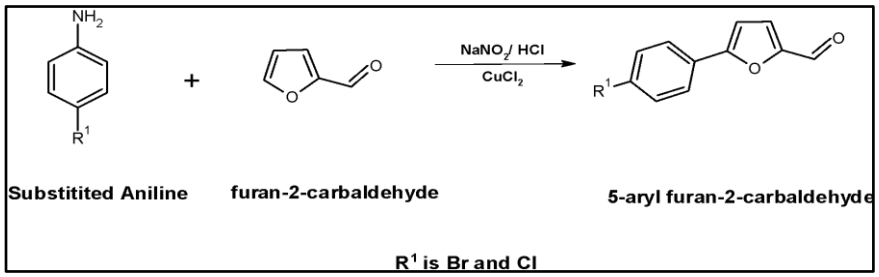

Fig. 1. Synthesis of 5-aryl furans.

2.4. *Weight loss method*

A 0.1 N HCl solution with and without different doses of the inhibitors was utilized for all the weight loss studies in a test tube. From 100 to 600 ppm, the concentrations were changed. A full day of soaking was required at room temperature. An hour of immersion at three distinct raised temperatures (323K, 333K, and 343K) was used to study the inhibitors' inhibitory activity. It was recorded the weight of the mild steel coupon before it was immersed in the appropriate solution. After each interval, the mild steel coupons were wiped with acetone, allowed to dry, and then their weights were recorded. The following formula was used to compute the corrosion rate (C.R) using the observed change in weights.

$$C.R = \frac{w}{S.t} \quad (1)$$

C.R is corrosion rate, W is the difference in the weight of mild steel, S is the surface area of the used specimen, and t is the immersion time in hours.

Inhibition percentage (IE%) was calculated by using the following equation

$$\text{IE (\%)} = \frac{C.R - C.R'}{C.R} \times 100 \quad (2)$$

Where $C.R$ and $C.R'$ are the corrosion rate of the mild steel sample in the absence and presence of the inhibitor.

Surface coverage (θ) was calculated by using the following equation

$$\theta = \frac{C.R - C.R'}{C.R} \quad (3)$$

2.5. *Electrochemical analysis*

The open circuit potential (OCP) and potentiodynamic polarization curves were obtained using Squidstat Solo 2181, an electrochemical measuring device with corrosion method software from Admiral Instruments. Enamel lacquer was used to cover a 1 cm^2 working surface in order to conceal the polished mild steel coupons, and a little portion was left at the tip to facilitate electrical contact. Desiccation was used to dry the coupons. A Pyrex glass beaker with three necks was utilized for the experiment. A saturated calomel electrode served as the reference electrode, while graphite was employed as the counter electrode. The apparatus was connected to a Pyrex glass container that contained 100 cm^3 of the experimental solution; the reference electrode, counter electrode, and working electrode were all immersed in this liquid. Scanning the potentials from -0.25 V to 0.25 V was done at a rate of 5 mV/s. After an hour of running the open circuit potentials, a steady curve was achieved. The mild steel potentiodynamic polarization curves were subsequently derived.

2.6. *Surface analysis*

The study compared the metal surface's passive layer with and without an inhibitor solution at 600 ppm using scanning electron microscopy and energy dispersive X-ray analysis.

3. Results and Discussion

3.1. *Characteristics*

In order to evaluate the synthetic inhibitors' characteristics, we captured "The Fourier Transform Infrared Spectrum (FTIR)" from 500 to 4000 cm^{-1} with a 2 cm^{-1} resolution using a Perkin-Elmer 1710 spectrophotometer.

5-[4-bromophenyl]-furan-2-carbaldehyde Fig. 2a: Yield: 83.44 %, Melting Point: 149 - 151°C, FTIR (KBr cm^{-1}): 3095.75(=C-H), 1720.81(C=O), 1646.71(C=C), 1384(O=C-H),683.12(C-Br).

5-[4-chlorophenyl]-furan-2-carbaldehyde Fig. 2b: Yield: 80.21 %, Melting Point: 116-118 °C, FTIR (KBr cm^{-1}): 3090.27(=C-H), 1725.03(C=O), 1641.49(C=C), 1384.24(O=C-H), 756.69(C-Cl).

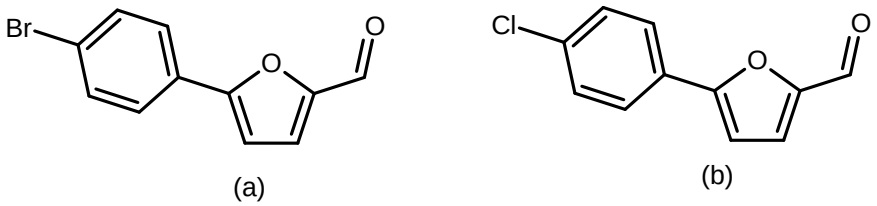

Fig. 2. (a) Structures of 5-[4-bromophenyl]-furan-2-carbaldehyde (BFC) and (b) 5-[4-chlorophenyl] furan-2-carbaldehyde (CFC).

3.2. *Weight loss analysis*

3.2.1. *Effect of concentration*

Table 1 shows the results of inhibiting mild steel corrosion at room temperature with increasing inhibitor concentrations for both inhibitors. The results demonstrated that the corrosion rate decreased when the quantity of both inhibitors was increased, suggesting that the inhibitors effectively reduced corrosion. The maximum inhibitory effectiveness for 5-[4-bromophenyl]-furan-2-carbaldehyde was 92.10 % at a concentration of 600 ppm, whereas for 5-[4-chlorophenyl]-furan-2-carbaldehyde it was 89.47 %. Both inhibitors adsorb to the metal surface, thereby preventing the active corrosion sites, which might explain this. As a result, the inhibition efficiency improves and the metal dissolution into the solution reduces [18,19]. The results showed that the inhibitor with the Br moiety was somewhat more effective than the one with the Cl moiety, according to the data. This is because Br^- has a bigger atomic radius than Cl^-, and because it has a synergistic impact in HCl media; also, the literature states that Br- ions are less electronegative than Cl- ions. This allows Br^- to outperform Cl^- ion in corrosion inhibition [20]. The relationship between corrosion rate and inhibition efficiency at various inhibitor doses is shown in Figs. 3a,b.

Table 1. Gravimetric analysis data of mild steel in 0.1 N HCL in the absence and presence of synthesized furan derivatives at room temperature.

5-[4-bromophenyl]-furan-2-carbaldehyde					5-[4-chlorophenyl]-furan-2-carbaldehyde			
Sr.no	C ppm	Inhibition Efficiency (I.E.%)	Corrosion Rate $mgcm^{-2}h^{-1}$	Surface Coverage θ	C ppm	Inhibition Efficiency (I.E.%)	Corrosion Rate $mgcm^{-2}h^{-1}$	Surface Coverage θ
01	Blank	-	0.220	-	Blank	-	0.220	-
02	100	47.36	0.116	0.47	100	52.63	0.104	0.52
03	200	55.26	0.098	0.55	200	63.15	0.081	0.63
04	300	78.94	0.046	0.78	300	71.05	0.063	0.71
05	400	86.84	0.029	0.86	400	78.94	0.046	0.78
06	500	89.47	0.023	0.89	500	84.21	0.034	0.84
07	600	92.10	0.017	0.92	600	89.47	0.023	0.89

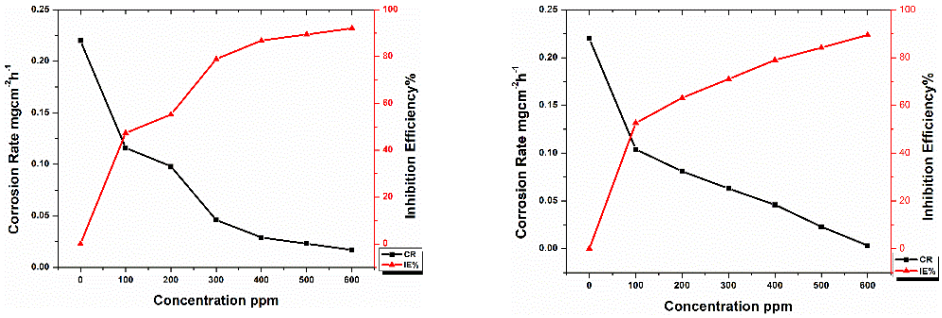

Fig. 3. (a) Corrosion rates and inhibition efficiencies at different concentrations of 5-[4-bromophenyl]-furan-2-carbaldehyde and (b) 5-[4-chlorophenyl]-furan-2-carbaldehyde.

3.2.2. *Effect of temperature on inhibitors*

Three raised temperatures (323K, 333K, and 343K) were used to study the inhibitory properties of the synthesized inhibitors. Table 2 lists the data that were gathered. The results showed that the corrosion rate was proportional to the temperature. Metals dissolve into solutions at higher temperatures because the kinetics of the anodic and cathodic processes are both improved. Both inhibitors acted at high temperatures to impede the mild steel. Raising the temperature from 323K to 343K reduced the inhibitory activity of both inhibitors. This occurs because, as the temperature increases, the adsorbed film is reabsorbed into the solution. As a result, corrosion begins to develop since there is now a hole in the passive coating that was previously present on the metal surface [21-27].

Table 2. Gravimetric analysis data for MS in the absence and presence of synthesized furan derivatives BFC & CFC respectively at 323 K, 333 K, and 343K.

5-[4-bromophenyl]-furan-2-carbaldehyde (BFC)							5-[4-chlorophenyl]-furan-2-carbaldehyde (CFC)					
	Corrosion rate (C.R) $mgcm^{-2}h^{-1}$			Inhibition Efficiency (η) %			Corrosion rate (C.R) $mgcm^{-2}h^{-1}$			Inhibition Efficiency (η) %		
Concentration ppm	323 K	333 K	343 K	323 K	333 K	343 K	323 K	333 K	343 K	323 K	333 K	343 K

0	6.545	7.799	8.913	-	-	-	6.545	7.799	8.913	-	-	-
100	2.22	3.064	3.62	65.95	60.71	59.37	1.81	2.51	4.32	72.34	67.85	51.56
200	1.53	2.50	3.06	76.59	67.85	65.6	1.53	2.09	3.34	76.59	73.21	62.5
300	0.97	1.82	2.64	85.10	76.7	70.31	0.97	1.81	2.50	85.7	76.7	71.87
400	0.55	1.39	1.94	91.48	82.14	78.12	0.69	1.39	1.81	89.36	82.14	79.68
500	0.27	0.69	1.25	95.74	91.07	85.9	0.27	0.83	1.53	95.2	89.28	82.81

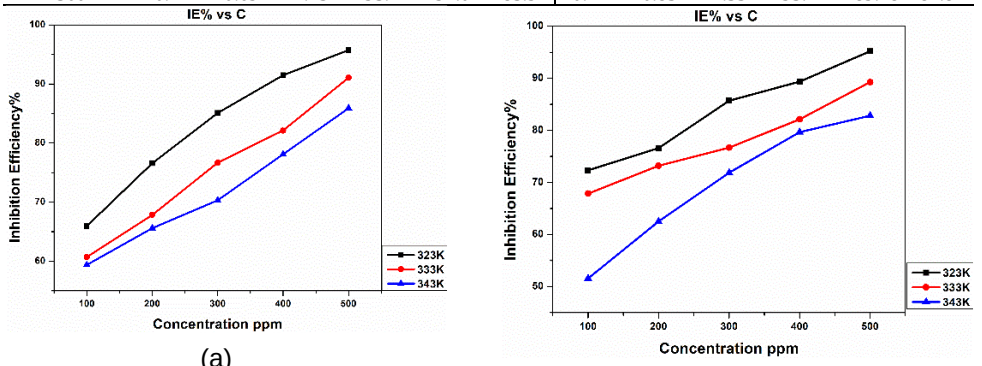

Fig. 4. (a) Correlation of inhibition efficiencies with the different concentrations of 5-[4-bromophenyl]-furan-2-carbaldehydeand and (b) 5-[4-chlorophenyl]-furan-2-carbaldehyde at various temperatures.

3.2.3. *Activation parameters*

The activation parameters of the corrosion process were calculated by using Arrhenius Eq (4)

$$\ln C.R = \ln A - \frac{Ea}{RT} \quad (4)$$

Where $C.R$ is the corrosion rate, Ea is the activation energy, R is the universal gas constant, A is the frequency factor and T is the absolute temperature.

According to the plots of ln C.R vs 1/T in Fig. 5, the activation energies (Ea) of the inhibitors are provided in Tables 3 and 4, respectively. Table 3 shows the values of the linear regression coefficient (R2) and straight lines for both inhibitors, suggesting a significant linear connection between ln $a.R$ and 1/T. Both inhibitors caused the inhibited molecules to have a greater activation energy compared to the uncontrolled ones. Furthermore, Ea values increased in tandem with inhibitor concentration. An increasing physical barrier between the acidic solution and the metal surface is produced by an increasing concentration of the inhibitor [25].

The activation enthalpy (ΔH) and activation entropy (ΔS), which were calculated using the alternate form of Arrhenius Eq (5), are listed in Table (3) and Table (4), respectively.

$$C.R = \frac{RT}{Nh} exp\left[\frac{\Delta S}{R}\right] exp\left[-\frac{\Delta H}{RT}\right] \quad (5)$$

The variables denoted by h, N, ΔS, ΔH, R, and T stand for Plank's constant, Avogadro's constant, activation of enthalpy, universal gas constant, and absolute temperature, specifically.

Fig. 6 display the graph of the natural logarithm of C.R/T against the inverse of absolute temperature 1/T. The values of (ΔH) and (ΔS) were found by taking the intercept of ln(R/Nh) + ΔS/R and the slopes of (-ΔH/R). The metal dissolves at a slower speed, a phenomenon called endothermic dissolution, because both inhibitors have a positive sign of (ΔH). Both inhibitors have negative (ΔS) values, which means an activated compound is formed in the rate-determining phase. As we get from the reactant to the activated complex, this indicates that the disorderliness increases [3,7].

Table 3. Activation Parameters data of mild steel in the presence of 5-[4-bromophenyl]-furan-2-carbaldehyde in 0.1 N HCl.

Sr.no	Concentration ppm	R^2	Ea kJ/mol	ΔH kJ/mol	$-\Delta S$ J/mol	ΔG kJ/mol			
						303K	323K	333K	343K
01	0	0.9977	13.89	10.87	196.12	70.26	74.18	76.14	78.10
02	100	0.9817	21.79	18.92	179.98	73.17	76.74	78.53	80.32
03	200	0.9610	30.73	27.89	155.22	74.86	77.96	79.51	81.06
04	300	0.9885	43.90	41.39	117.13	76.84	79.18	80.35	81.52
05	400	0.9590	55.17	52.84	86.10	78.89	80.61	81.47	82.33
06	500	0.9907	66.84	64.62	55.65	81.29	82.60	83.15	83.71

Table 4. Activation Parameters data of mild steel in the presence of 5-[4-chlorophenyl]-furan-2-carbaldehyde in 0.1 N HCl.

Sr.no	Concentration ppm	R^2	Ea kJ/mol	ΔH kJ/mol	$-\Delta S$ J/mol	ΔG kJ/mol			
						303K	323K	333K	343K
01	0	0.9977	13.58	10.87	196.12	73.00	74.21	76.17	78.13
02	100	0.9952	37.82	31.39	144.87	75.28	78.18	79.63	81.08
03	200	0.9786	33.97	35.19	131.78	75.11	77.75	79.07	80.39
04	300	0.9779	41.67	39.24	124.22	76.87	79.36	80.60	81.84
05	400	0.9502	42.47	39.85	124.51	77.57	80.06	81.31	82.55
06	500	0.9811	76.24	73.61	27.602	81.97	82.52	82.80	83.07

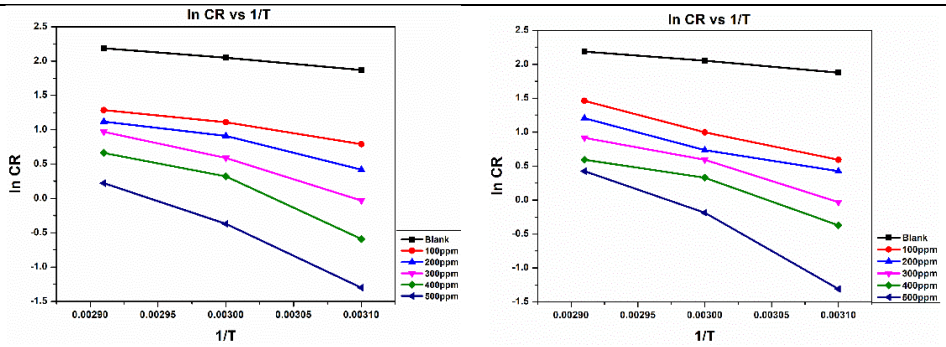

Fig. 5. (a) Arrhenius diagrams for mild steel corrosion in acidic solution in the presence and absence of different concentrations of (a) 5-[4-bromophenyl]-furan-2-carbaldehyde and (b) 5-[4-bromophenyl]-furan-2-carbaldehyde.

The change in free energy of activation was calculated using Eq (6)

$$\Delta G = \Delta H - T\Delta S \quad (6)$$

Tables 3 and 4 include the computed ΔG values. As the temperature and concentration of the inhibitors rose, it was noted that the ΔG values were positive and increased for both of them. When heated to higher degrees, the activated chemical becomes unstable and corrosion starts to happen on its own. At higher temperatures, the rate of corrosion increases due to the desorbed inhibitor going back into the solution [28].

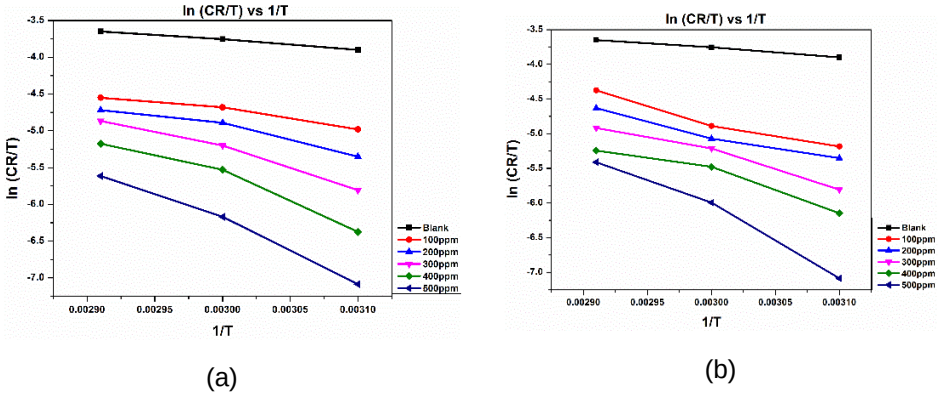

Fig. 6. Transition State plots for mild steel in acidic solutions in the absence and presence of different concentrations of (a) 5-[4-bromophenyl]-furan-2-carbaldehyde and (b) 5-[4-chlorophenyl]- furan-2-carbaldehyde.

3.3.4. *Adsorption isotherm*

To find the adsorption isotherm, the surface coverage (θ), which was discovered using gravimetric measurement, was consumed. The isotherm analysis provides insight into the inhibitor's metal-surface interaction. Langmuir Adsorption isotherms were determined to be the most appropriate match for the data acquired for both inhibitors after analysing all the possible adsorption isotherms.

$$\frac{C}{\theta} = \frac{1}{k_{ads}} + c \quad (7)$$

Table 1 lists the variables C, which represents the inhibitor concentration, Kads, which stands for the absorptive equilibrium constant, and θ, which stands for the surface coverage. In Fig. 7 Langmuir plot (C/θ vs C) is illustrated. The inhibitors' regression values (R^2) and their slopes are given in Tables 5 and 6. Both graphs adhere to the Langmuir adsorption isotherm since the data is linear and the slope values are closer to one. Furthermore, the (R^2) values are close to 1, suggesting a strong agreement with the Langmuir isotherm. The y-intercept of the C/θ vs. C plot was used to compute the adsorption coefficient constant (Kads), which is provided in Tables 5 and 6. Findings from the weight loss approach were in accordance with the inhibitors' adsorption constants, which reduced with increasing temperature. In addition, 5-[4-bromophenyl] has a (Kads) value.5-[4-chlorophenyl]-furan-

2-carbaldehyde has a higher (Kads) value. This agrees well with the gravimetric results as well as -furan-2-carbaldehyde [29].

The standard free energy of adsorption (ΔG^0_{ads}) listed in Tables 5 and 6 was calculated by using Eq (8)

$$(\Delta G^0_{ads}) = -RT \ln (55.5\ K_{ads}) \quad (8)$$

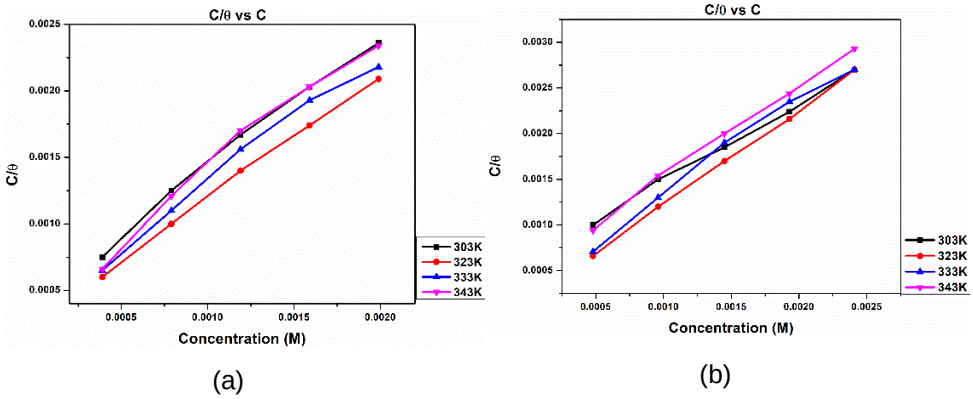

Fig. 7. Langmuir adsorption plots for mild steel surface in acidic solution at different temperatures for (a) 5-[4-bromophenyl]-furan-2-carbaldehyde and (b) 5-[4-chlorophenyl]-furan-2-carbaldehyde.

Both inhibitors showed signs of spontaneous adsorption due to their negative (ΔG^0ads) values. According to the literature, with values of (ΔG^0ads) about -20 kJ/mol, physisorption happens when there is an electrostatic attraction between the charged inhibitor molecule and the charged metal surface. However, chemisorption happens when the iron molecule's d-orbital and the inhibitor's electrons combine to establish a coordinate kind of bond, as shown by values as high as -40 kJ/mol. In the case of 5-[4-bromophenyl]-furan-2-carbaldehyde, the (ΔG0ads) values varied between -29.43 kJ/mol and -34.19 kJ/mol, whereas those for 5-[4-chlorophenyl]-furan-2-carbaldehyde were -28.80 kJ/mol and -33.12 kJ/mol, respectively. This points to the usage of mixed-type inhibitors, which means that physical and chemical adsorption are both involved in the inhibitory process [30-33].

Table 5. Thermodynamic adsorption parameters of 5-[4-bromophenyl]-furan-2-carbaldehyde at different temperatures.

Sr. no	Temperature K	R^2	Slope	K_{ads}	$-\Delta G^0_{ads}$ kJ/mol	ΔH^0_{ads} kJ/mol	ΔS^0_{ads} J/mol
01	303	0.9908	0.95	2141.3	29.43		
02	323	0.9985	0.93	3861	32.96		
03	333	0.9877	0.97	3333.3	33.57	-12.42	63.53
04	343	0.9830	1.04	2906.9	34.19		

Table 6. Thermodynamic adsorption parameters of 5-[4-chlorophenyl]-furan-2-carbaldehyde at different temperatures.

Sr. no	Temperature K	R^2	Slope	K_{ads}	$-\Delta G^0_{ads}$ kJ/mol	$\Delta H^0_{a\,ds}$ kJ/mol	$\Delta S^0_{a\,ds}$ J/mol
01	303	0.9966	0.85	1666.6	28.80		
02	323	0.9993	1.043	5000	33.65		
03	333	0.9887	1.04	3333.3	33.57	-40.008	86.395
04	343	0.9967	1.01	2000	34.12		

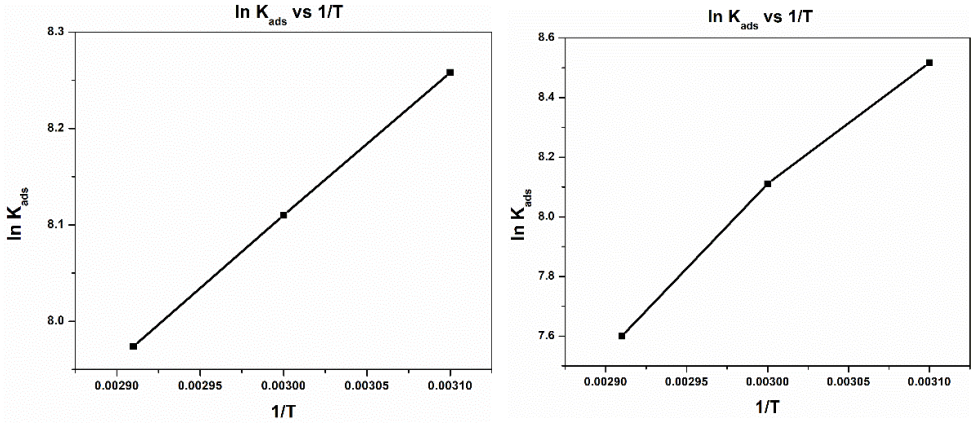

Fig. 8. (a) Van't Hoff plots of mild steel in 0.1N HCl solution for (a) 5-[4-bromophenyl]-furan-2-carbaldehyde and (b) 5-[4-chlorophenyl]-furan-2-carbaldehyde.

Adsorption enthalpy (ΔH^0_{ads}) and adsorption entropy (ΔS^0_{ads}) was calculated using the Van't Hoff Equation (9). The values of (ΔH^0_{ads}) and (ΔS^0_{ads}) are listed in Tables 5 and 6.

$$\ln K_{ads} = -\frac{\Delta H^0_{ads}}{RT} + \frac{\Delta S^0_{ads}}{R} + ln\frac{1}{55{\cdot}5} \quad (9)$$

From the plot of ln K_{ads} Vs 1/T (Figs. 8a,b) the values of $\Delta H^0_{a\,ds}$ and $\Delta S^0_{a\,ds}$ are calculated from the slope and the intercept respectively. It was determined that the adsorption process was exothermic since the value of $\Delta H_{a_{ds}}$. was negative for both inhibitors. It appears that the efficiency of the inhibition diminishes as the temperature rises. This occurs because the inhibitor that was applied desorbs at higher temperatures. The entropy of the system rises throughout the adsorption process, as shown by the positive value of ΔS_{ads} [32,33].

4. Electrochemical Analysis

4.1. *Open circuit potential*

It was observed, how the open circuit potential changed with and without varying amounts of the two inhibitors. The OCP curves that were produced are shown in Figs. 9a and 9b, respectively. After 30 min of immersion, the potential was found to have stabilized". At the

steady state, $I_{ox}=I_{red}$, and the potential is considered to be zero. In contrast to the inhibited mild steel sample, whose steady-state potential leaned more towards the positive side, the uninhibited mild steel sample exhibited a greater negative steady-state potential. This beneficial transformation is due to passivation of metal, which occurs when the inhibitor in use adsorbs onto the surface of the mild steel. There was a positive shift in the steady-state potential towards the positive side as inhibitor concentration increased. If the inhibitors have improved the mild steel's anodic process, then the steady-state potential has changed for the better [34,35].

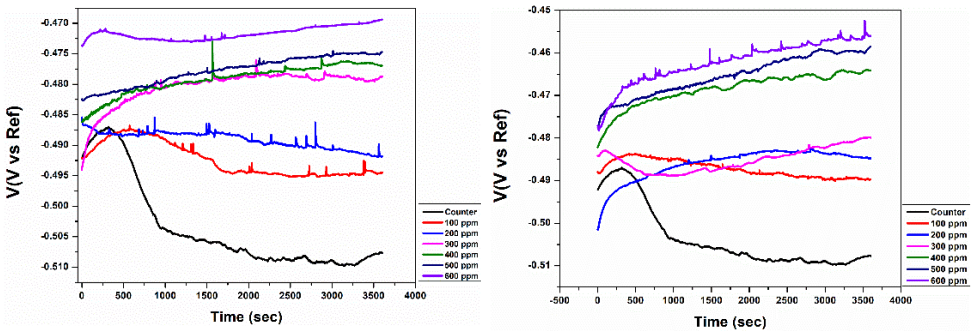

Fig. 9. Open Circuit Potential Plots of Mild Steel in acidic solution in the absence and presence of (a) 5-[4-bromophenyl]-furan-2-carbaldehyde and (b) 5-[4-chlorophenyl]-furan-2-carbaldehyde.

4.2. *Potentiodynamic polarization*

The polarization graphs for the two inhibitors utilized are shown in Fig. 10, respectively. The electrochemical properties, such as corrosion current (Icorr), corrosion potential (Ecorr), cathodic Tafel slope (βc), and anodic Tafel slope (βa), that were found by extrapolating the Tafel curves are presented in Tables 7 and 8. Equation 10 was used to compute the inhibitory efficiency.

$$IE\% = \frac{icorr - icorr'}{icorr} \text{ X } 100 \qquad (10)$$

Where i_{corr} is the corrosion current densities of uninhibited mild steel and i_{corr}' is the corrosion current densities in the presence of the inhibitor.

Both inhibitors' corrosion current densities declined with increasing inhibitor concentration, according to the results. Accordingly, the inhibitors used moved the cathodic and anodic Tafel slopes in the direction of reduced current densities. Both inhibitors greatly reduced corrosion rate, enhancing inhibition efficiency. A cathodic or anodic inhibitor is defined as one in which the corrosion potential difference between an unfettered mild steel sample and any inhibited sample is more than -85 mV, as stated in the literature. For 5-[4-bromophenyl]-furan-2-carbaldehyde, the Ecorr values were as small as 10 mV, while for 5-[4-chlorophenyl]-furan-2-carbaldehyde, the greatest difference was 29 mV. This proves that

the inhibitors utilized are a combination of different types. The mild steel surface is protected by the inhibitors because they change the cathodic and anodic processes. In the absence of any discernible shift in Ecorr values, the adsorption process may go on purely as a blocking mechanism. While the blocking impact is more prominent, the Ecorr values did vary for both inhibitors, suggesting that the inhibitors also changed the activation energies of cathodic and anodic processes [36-38].

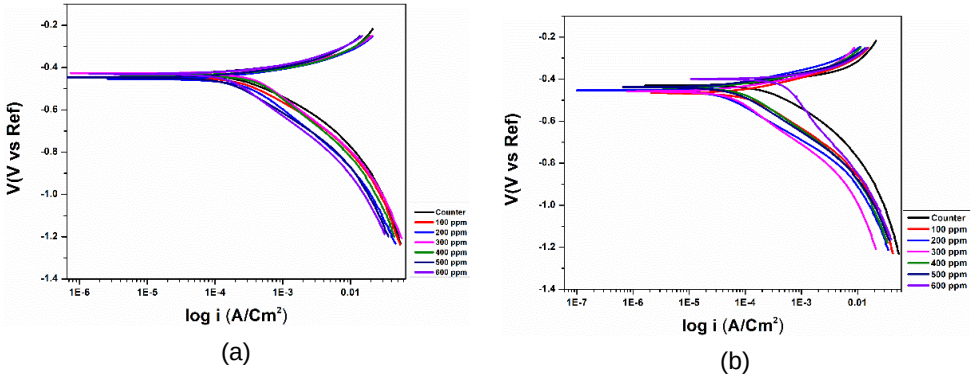

Fig. 10. Tafel's plots for mild steel in an acidic solution in the presence and absence of (a) 5-[4-bromophenyl]-furan-2-carbaldehydeand (b) 5-[4-bromophenyl]-furan-2-carbaldehyde.

Table 7. Potentiodynamic polarization parameters for the corrosion of mild steel in 0.1 N HCl without and with different concentrations of 5-[4-bromophenyl]-furan-2-carbaldehyde.

Sr.no	Concentration ppm	βa 10^{-3} (V/dec)	βc 10^{-3} (V/dec)	i_{corr} μA	$-E_{corr}$ mV	CR mpy	Inhibition Efficiency %
01	0	126	281	409	434	187.15	-
02	100	65.9	187	215	440	98.5	47.43
03	200	51.1	203	189	444	86.28	53.78
04	300	43.1	199.1	146	424	66.58	64.30
05	400	23.3	158.9	107	434	49.25	73.83
06	500	20.0	161.7	45.9	443	21.03	88.75
07	600	14.2	139	30.0	428	13.75	92.66

Table 8. Potentiodynamic polarization parameters for the corrosion of mild steel in 0.1 N HCl without and with different concentrations of 5-[4-chlorophenyl]-furan-2-carbaldehyde.

Sr. no	Concentration ppm	βa 10^{-3} (V/dec)	Bc 10^{-3} (V/dec)	i_{corr} μA	$-E_{corr}$ mV	CR mpy	Inhibition Efficiency %
01	0	126	281	409	434	187.15	-
02	100	85.4	210	172	463	78.80	57.94
03	200	90.1	232	124	447	56.73	69.68
04	300	74.3	235	98.9	459	45.31	75.84
05	400	58.2	184	79.7	439	36.48	80.51
06	500	47.9	177	56.2	430	25.72	86.25
07	600	30.7	109	36.3	438	13.23	91.12

5. Surface analysis

5.1. *SEM analysis*

The passive layer formed on the metal surface was examined using scanning electron microscopy. Fig. 11 show different scanning electron micrographs (SEM) of the polished mild steel sample before, during, and after immersion in acidic solutions (0.1 N HCl), 600 ppm of 5-[4-bromophenyl]-furan-2-carbaldehyde, and 600 ppm of 5-[4-chlorophenyl]-furan-2-carbaldehyde, respectively. The mild steel coupon had a flat surface before being immersed in the acidic solution, as shown in Fig. 11a. But pits and fractures start to emerge after a day of exposure in acidic conditions. The metal coupon is therefore being destroyed. Figs. 11c,d show that when both inhibitors are present, the surface remains smooth and free of pits and fissures. It is evident that the inhibitor in question has successfully attached to the metal surface and created a protective coating [36-38].

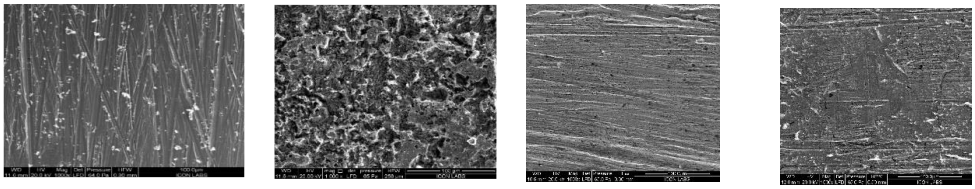

Fig. 11. SEM images of mild steel, a: before immersion in acidic solution, b: after immersion in acidic solution for 24 hours, c: after immersion in acidic solution in the presence of 5-[4-bromophenyl]-furan-2-carbaldehyde, d: after immersion in acidic solution in the presence of 5-[4-chlorophenyl]-furan-2-carbaldehyde.

5.2. *EDAX analysis*

The surfaces of inhibited and uninhibited mild steel were compared using EDAX analysis. Polished mild steel in the presence of 600 ppm 5-[4-bromophenyl]-furan-2-carbaldehyde and polished mild steel before and after immersion in 0.1 N HCl solution for 24 h are shown in Figs. 12a-d, respectively, in the EDAX spectra. The elemental compositions are listed in Tables 9 and 10.

Table 9. Chemical composition of mild steel in 0.1 N HCl in the presence and absence of 5-[4-bromophenyl]-furan-2-carbaldehyde.

Medium	Composition %				
	Iron	Oxygen	Chlorine	Carbon	Bromine
Polished (11A.)	89.9	-	-	9.0	-
0.1N HCl (11B.)	62.9	16.7	0.8	10.6	-
600 ppm of BFC (11C.)	79.5	8.2	-	29.3	2.8

Table 10. Chemical composition of mild steel in 0.1 N HCl in the presence and absence of 5-[4-chlorophenyl]-furan-2-carbaldehyde.

Medium	Composition %			
	Iron	Oxygen	Chlorine	Carbon
Polished (11A.)	89.9	-	-	9.0
0.1N HCl (11B.)	62.9	16.7	0.8	10.6
600 ppm of CFC (11C.)	72.7	13.7	1.1	32.8

Tables 9 and 10 show that the iron content of the mild steel was around 90 % when it was first produced. The reduction to 62 % was seen after immersion in a solution of 0.1 N HCl. In addition, before being immersed in an acidic media, there was no chlorine or oxygen content. The higher iron level is clearly caused by the presence of the inhibitors after immersion in 600 ppm of the relevant compounds. When 5-[4-bromophenyl]-furan-2-carbaldehyde is present, a new bromine peak is also visible. This demonstrates that the inhibitor successfully prevented adsorption and formed a protective coating on the surface of the metal. The presence of 5-[4-chlorophenyl]-furan-2-carbaldehyde raises the chlorine concentration because the chlorine atom of the inhibitor is adsorbed onto the surface of the metal to protect it from acidic conditions [36,39,41].

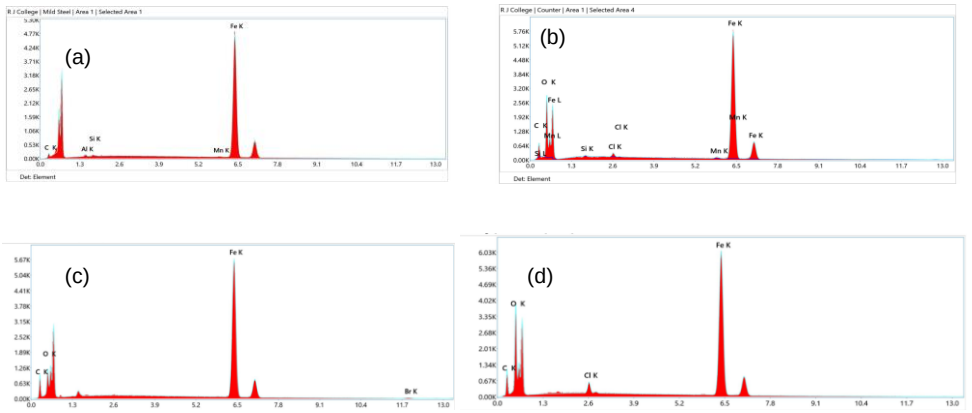

Fig. 12. EDAX analysis of mild steel, a: before immersion in acidic solution, b: after immersion in acidic solution for 24 h, c: after immersion in acidic solution in the presence of 5-[4-bromophenyl]-furan-2-carbaldehyde, d: after immersion in acidic solution in the presence of 5-[4-chlorophenyl]-furan-2-carbaldehyde.

6. Mechanism of Inhibition

The factors that determine the inhibitor's ability to be adsorbed include acid content, ambient factors, metal type, inhibitor size, adsorption centre, and inhibitor structure. The literature indicates that there are two forms of inhibitor adsorbed on metal surfaces. First, a chemisorption method is used to adsorb the neutral molecule onto the surface of the metal. This occurs when water molecules depart from the mild steel's surface and come into

contact with the iron's surface, where a heteroatom with two electrons occupies the vacant d-orbital. The inhibitor might be adsorbed onto the metal surface through interactions with the pi-electrons of the phenyl ring. Use the positive charge on the metal surface to attract the negatively charged inhibitor, which is the second way around. The two inhibitors in this study are adsorbed by interacting with the vacant d-orbital of the iron surface through a donor-acceptor process involving the pi-electrons of heteroatoms. Additionally, the inhibitor's bromine and chlorine atoms, which are negatively charged, may be electrostatically attracted to the positively charged metal surface and adsorb to it [41,42].

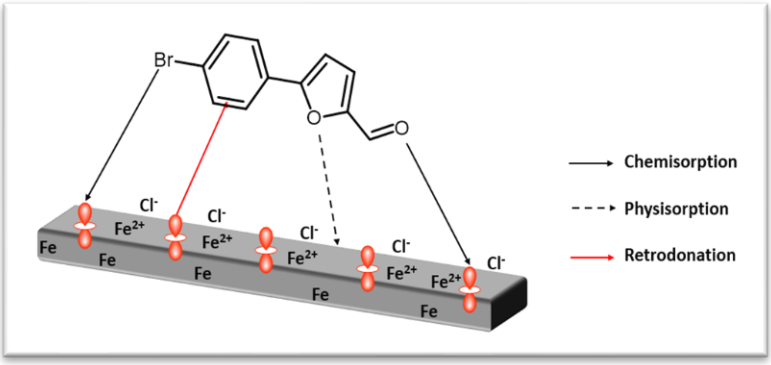

Fig. 13. Corrosion mitigation mechanism of 5-[4-bromophenyl]-furan-2-carbaldehyde.

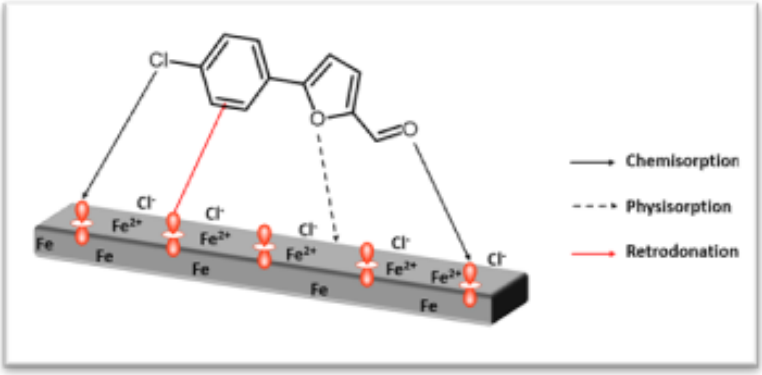

Fig. 14. Corrosion mitigation mechanism of 5-[4-chlorophenyl]-furan-2-carbaldehyde.

7. Conclusion

Furan derivatives in a 0.1N HCl solution, 5-[4-bromophenyl]-furan-2-carbaldehyde and 5-[4-chlorohenyl]-furan-2-carbaldehyde inhibited mild steel corrosion. The data demonstrate that both inhibitors were effective at blocking the action of the target compounds; at 600 ppm, 5-[4-bromophenyl]-furan-2-carbaldehyde had an efficiency of 92.10 % and 5-[4-chlorohenyl]-furan-2-carbaldehyde 89.47 %. Because of the synergistic action of the

bromine atom, 5-[4-bromophenyl]-furan-2-carbaldehyde showed somewhat greater efficiency. For both inhibitors, it was noted that the efficacy of inhibition decreased with increasing temperature. Physical and chemical adsorption were both aided by the inhibitors. Both the studied inhibitors were observed to follow the Langmuir Adsorption Isotherm. It was determined via electrochemical research that the inhibitors used are a mixture of several sorts. The existence of a passive coating, which prevents corrosion on mild steel surfaces, was verified by surface analysis.

References

1. M. G. Fontana, Corrosion Engineering, 3rd Edition (McGraw Hill Book Company, New York, 1986).
2. J. K. Odusote and O. M. Ajayi, J. Electrochem. Sci. Technol. **4**, 81 (2013). https://doi.org/10.5229/JECST.2013.4.2.81
3. A. M. Ashmawy, M. A. Mostafa, A.-B. Kamal, G. M. Ali, and M. S. A. El-Gaby, Sci. Rep. **13**, ID 18555 (2023). https://doi.org/10.1038/s41598-023-45659-2
4. M. Erna, H. Herdini, and D. Futra, Int. J. Chem. Eng. **2019**, ID 514132 (2019). https://doi.org/10.1155/2019/8514132
5. M. E. Azhar, B. Mernari, M. Traisnel, F. Bentiss, and M. Lagrenée, Corrosion Sci. **43**, 2229 (2001). https://doi.org/10.1016/S0010-938X(01)00034-8
6. P. Raotole, R. S. Khadayte, and V. Huse, Int. J. Creat. Res. Thoughts (IJCRT) **10**, 636 (2022).
7. A. O. Okewale and O. A. Adesina, J. Appl. Sci. Environ. Manag. **24**, 37 (2020). https://doi.org/10.4314/jasem.v24i1.6
8. G. S. Sajadi, R. Naghizade, L. Zeidabadinejad, Z. Golshani, M. Amiri et al., Heliyon **8**, ID e10983 (2022). https://doi.org/10.1016/j.heliyon.2022.e10983
9. M. H. Mahross, K. Efil, T. A. S. El-Nasr, and O. A. Abbas, J. Electrochem. Sci. Technol. **8**, 222 (2017). https://doi.org/10.33961/JECST.2017.8.3.222
10. S. Shahen, Al-Azhar Bull. Sci. **30**, 47 (2019). https://doi.org/10.21608/absb.2019.67892
11. D. Prakash, R. K. Singh, and R. Kumari, Ind. J. Chem. Technol. **13**, 555 (2006).
12. M. Alizadeh, M. Jalal, K. Hamed, A. Saber, S. Kheirouri et al., J. Inflam. Res. **13**, 451 (2020). https://doi.org/10.2147/JIR.S262132
13. H. Saeid, H. Al-sayed, and M. Bader, Alq. J. Med. Appl. Sci. **6**, 44 (2023). https://doi.org/10.5281/zenodo.7650255
14. H. A. Ali, A. A. El-Hossiany, A. S. Abousalem, M. A. Ismail, A. E-A. S. Fouda, et al., BMC Chem. **18**, ID 182 (2024). https://doi.org/10.1186/s13065-024-01280-6
15. A. M. Al-Fakih, H. H. Abdallah, and M. Aziz, Mater. Corrosion **70**, 135 (2018). https://doi.org/10.1002/maco.201810221
16. S. Aslam, A. Nazeer, M. N. Khan, N. Parveen, M. A. Khan et al., Asian J. Chem. **25**, 9595 (2013). https://doi.org/10.14233/ajchem.2013.15091
17. K. Subrahmanya and B. S. Holla, Heterocyclic Commun. **9**, 625 (2003). https://doi.org/10.1515/hc.2003.9.6.625
18. J. D. Amine, T. J. Ikyuve, and A. Ashwe, J. Mater. Sci. Metallurgy **4,** 1 (2023).
19. O. Abdellaoui, M. K. Skalli, A. Haoudi, Y. K. Rodi, N. Arrousse et al., Moroccan J. Chem. **9,** 43 (2021). http://dx.doi.org/10.48317/IMIST.PRSM/morjchem-v9i1.21313
20. Z. Yang, C. Qian, W. Chen, M. Ding, Y. Wang et al., Colloids Interface Sci. Commun. **34**, ID 100228 (2020). https://doi.org/10.1016/j.colcom.2019.100228
21. A. Sehmi, H. B. Ouici, A. Guendouzi, M. Ferhat, O. Benali et al., J. Electrochem. Sci. Technol. **167**, 155508 (2020). https://doi.org/10.1149/1945-7111/abab25
22. Key Heterocycle Cores for Designing Multitargeting Molecules, ed. O. Silakari (Elsevier Ltd., 2018). https://doi.org/10.1016/C2016-0-01252-4
23. G. M. Ziarani, R. Moradi, T. Ahmadi, and N. Lashgari, Royal Soc. Chem. **8** (2018).

24. E. D. Morgan, Endeavour **14**, 148 (1990). https://doi.org/10.1016/0160-9327(90)90017-L
25. G. Karthik and M. Sundaravadivelu, Egyptian J. Petroleum **25**, 183 (2016). https://doi.org/10.1016/j.ejpe.2015.04.003
26. A. Nahlé, I. I. Abu-Abdoun, and I. Abdel-Rahman, Int. J. Corrosion **2012**, 1 (2012). https://doi.org/10.1155/2012/380329
27. B. S. Mahdi, M. K. Abbass, M. K. Mohsin, W. K. Al-azzawi et al., Molecules **27**, 4857 (2022). https://doi.org/10.3390/molecules27154857
28. A. F. S. A. Rahiman and S. Sethumanickam, Arabian J. Chem. **10**, S3358 (2017). https://doi.org/10.1016/j.arabjc.2014.01.016
29. L. A. Nnanna, K. O. Uchendu, F. O. Nwosu, U. Ihekoronye, and E. P. Eti, Int. J. Mater. Chem. **4**, 34 (2014). https://doi.org/10.5923/j.ijmc.20140402.03
30. R. K. Dubey, N. Gupta, S. M. Nafees, and K. S, Nature, Nature, Environ. Poll. Technol. **19**, 799 (2020). https://doi.org/10.46488/NEPT.2020.v19i02.037
31. P. P. Kamble and R. S. Dubey, Corcon Mumbai (2017). https://icspl.org/Corcon%202017/html/PDF/PP1.pdf
32. D. Q. Huong, T. Duong, and P. C. Nam, ACS Omega **4**, 14478 (2019). https://doi.org/10.1021/acsomega.9b01599
33. G. Gómez-Sánchez, O. Olivares-Xometi, P. Arrellanes-Lozada, N. V. Likhanova, I. V. Lizanova et al., Int. J. Mol. Sci. **24**, 6291 (2023). https://doi.org/10.3390/ijms24076291
34. J. D. Girase and R. S. Dubey, Int. J. Sci. Res. Sci., Eng., Technol. **5**, 48 (2018).
35. J. D. Girase, Corcon Mumbai (2016). https://icspl.org/Corcon%202017/html/PDF/MCI44.pdf
36. N. N. Bastam, H. R. H. Atabak, F. Atabaki, M. Radvar, and S. Jahangiri, Iranian J. Chem. Chem. Eng. **39**, 113 (2020)
37. P. P. Kamble and R. S. Dubey, J. Sci. Res. **13**, 979 (2021). http://dx.doi.org/10.3329/jsr.v13i3.52725
38. G. D. Girase, P. P. Kamble and R. S. Dubey, J. Sci. Res. **14**, 607 (2022). http://dx.doi.org/10.3329/jsr.v14i2.56113
39. D. G. Jitendra, K. Pratap, and R. S. Dubey, Int. Res. J. Sci. Eng. **A11**, 117 (2021).
40. A. Al-Amiery, A. Kadhum, A. H. Alobaidy, A. Mohamad, and P. Hoon, Materials **7**, 662 (2014). https://doi.org/10.3390/ma7020662
41. P. Kamble and R. S. Dubey, J. Sci. Res. Banaras Hindu University **65**, 55 (2021). https://doi.org/10.37398/jsr.2021.650607
42. V. Pinto, G. M. Pinto, L. D. Kateel, and A. Thomas, Biointerface Res. Appl. Chem. **13,** ID 544 (2023). https://doi.org/10.33263/BRIAC136.544